Clinical and Experimental Health Sciences

Effects of Contrast Limited Adaptive Histogram Equalization (CLAHE) on Manual and Automated Tracing of Lateral Cephalometric Radiographs

Merve Gonca[1], Çiğdem Sazak Turgut[2], Şeyma Gündoğdu[3]

[1] Recep Tayyip Erdoğan University, Faculty of Dentistry, Department of Orthodontics, Rize, Türkiye.
[2] Recep Tayyip Erdoğan University, Department of Computer Engineering, Rize, Türkiye.
[3] Istanbul Rumeli University, Vocational School of Health Services, İstanbul, Türkiye.

Correspondence Author: Merve Gonca
E-mail: mervegonca@gmail.com

Received: 08.09.2023 **Accepted:** 20.06.2024

ABSTRACT

Objective: The aim of this study is to compare the difference between original lateral cephalometric radiographs (LCRs) and Contrast Limited Adaptive Histogram Equalization (CLAHE) LCRs in two examiners and WebCeph.

Methods: A total of 200 LCRs were selected, and CLAHE (tile size: 20*20) was applied to the original LCRs. 27 LCR landmarks were manually determined by two examiners and, the selected LCR's determined automatically using the WebCeph program. Absolute differences between the original LCRs and CLAHE-LCRs were calculated in the x-y axes and Euclidean distance. The Kruskal Wallis test was used for comparisons between the examiners and WebCeph. The Wilcoxon Signed Rank Test was used to evaluate the x and y axes within each group.

Results: The best accuracy values were seen in examiner 1 along the x-y axes and Euclidean distance, while the worst accuracy values were seen in WebCeph. The mean differences according to the methods were higher along the y-axis than along the x-axis for both examiners (except PNS, Me') and WebCeph (except Po, Co). The mean Euclidean distances were above 2 mm only in Co, PNS at Examiner 1, PNS, Po, Ba, Co, Go, Pog, U1RT, Me', Pog at Examiner 2, and WebCeph in all measurements. However, the differences in Euclidean distances were less than 4 mm for both examiners and WebCeph.

Conclusion: CLAHE-LCRs require more adjustments for landmark determination in WebCeph than the in the manual system.

Keywords: Orthodontics; radiography; cephalometry; image enhancement; artificial intelligence; diagnostic imaging

1. INTRODUCTION

Lateral cephalometric radiographs (LCRs) are an essential evaluation tool in orthodontics, providing clinicians with information about dental and facial morphology. Changes during and post-treatment, tooth movements, facial growth, the relationship between the maxilla and mandible with the cranium, and the soft tissue profile are evaluated with LCR (1). The LCR landmarks are identifiable points that signify anatomical structures of hard or soft tissue. The structures are used as LCR landmarks for the determination of different cephalometric angles and measures (2).

Artificial intelligence (AI) is a machine's ability to mimic rational human behavior, including complex tasks (3). AI is becoming more widespread and reducing human performance requirements. Dentistry's applications have also significantly advanced. Dentists use AI algorithms to evaluate medical imaging and plan treatments (4,5). A significant development in orthodontics is the automatic identification of LCR landmarks to aid in diagnosing and treating dental and skeletal discrepancies (2). Several authors have used AI algorithms designed for a specific study and web-based software on search engines and mobile apps to study the accuracy of crucial landmark detection in cephalometric analysis. The studies compared AI algorithms' accuracy in localizing cephalometric landmarks on LCRs to manual tracing and examined algorithm differences. CephX, Ceppro, AudaxCeph, WebCeph, CephNinja, CS imaging V8, and CephNet are Commercial Software/Applications (6).

To ensure the accuracy of measurements as a diagnostic tool, it is essential to have high-quality LCRs and accurately marked anatomical landmarks. However, because of the intricate nature of the craniofacial region, there are challenges in identifying these landmarks, such as superimposition on two-dimensional images and variations in dentofacial morphology (7). Identification errors arise from the ability

DOI: 10.33808/clinexphealthsci.1357008

to identify anatomical landmarks in the correct localization. Improving the image quality of LCRs can significantly reduce these errors and improve the accuracy of identifying landmark localization (8,9). Therefore, it is crucial to strive for high-quality LCRs and accurate identification of anatomical landmarks to ensure reliable diagnostic information in orthodontic evaluations (10).

Image enhancement is a widely used technique in medical imaging systems to improve the quality of medical images. The use of image enhancement techniques can improve the quality of radiological images, allowing for more accurate and effective diagnosis (11). Histogram-based algorithms, such as Contrast-Limited Adaptive Histogram Equalization (CLAHE), are popular techniques for improving image contrast, brightness, and details (12). These contrast enhancement techniques not only aid in the assessment of radiographs by dentists but also function as a preliminary step for sophisticated automatic identification schemes based on deep learning methodologies (13). Most of the studies in the literature studied the point localization of experts as ground truth and compared it with AI-based programs how efficient they are (7,14). On the contrary, the main goal of our study was to compare the response of both the examiners and the AI-based program in differences between original and CLAHE LCRs, rather than ground truth-based evaluation.

2. METHODS

This retrospective study was approved by the research ethics committee of Recep Tayyip Erdogan University (number: 2021/168) and utilized LCRs obtained from patients referred for orthodontic treatment at the University's Department of Orthodontics in the Faculty of Dentistry. The LCRs were acquired using a Planmeca Promax 2D S2 device (Planmeca Oy; Helsinki, Finland) with exposure parameters set at 66 kVp, 10 mA, and 10.5 s. LCRs were obtained by the same technician.

Informed written consent forms were obtained from all patients at the beginning of their treatment, allowing their records to be used in scientific studies. Patients with the following features were selected from the orthodontic archive: a) in permanent dentition, b) no radiographs with projection errors, c) no individuals with craniofacial deformity, d) no individuals with impacted teeth or hypodontia, e) no presence of foreign body causing image artifact, f) no orthodontic attachments in the mouth and g) LCRs in which soft tissue was visible by both examiners.

Two orthodontists, one with ten and one with five years of clinical experience, analyzed the LCRs of 553 patients. A total of 353 LCRs that did not meet the inclusion criteria were excluded. In total, 200 LCRs were assessed in this study.

2.1. CLAHE Method

CLAHE is an image processing technique that enhances the image contrast while mitigating the amplification of noise and artifacts (15). Unlike traditional histogram equalization, which can produce unnatural results, CLAHE achieves this by dividing the image into smaller tiles and equalizing the histogram of each tile individually. A contrast limit was imposed on each tile to prevent over-amplification (12).

The optimal tile size depends on image characteristics, such as resolution and contrast properties. Smaller tiles enhance local contrast but may introduce graininess, whereas larger tiles smooth out noise but may reduce local contrast and detail. The optimal tile size depends on image characteristics, such as resolution and contrast properties. Images with low spatial frequencies generally benefit from larger tile sizes, whereas images with high spatial frequencies may require smaller ones. Dental tissues have small sizes and varied densities, requiring a delicate balance between contrast, detail, and artifact reduction (16). The visibility of soft tissues, such as organs or muscles, must be improved while retaining the contrast and reducing noise. When enhancing different tissues, tradeoffs are frequently encountered. CLAHE is a technique for achieving an acceptable balance by increasing local contrast (17). One method for addressing tradeoffs is selecting different enhancing techniques based on the region of interest. Adaptive approaches, such as CLAHE, can improve skeletal and dental tissues while maintaining the natural appearance of soft tissues and optimize overall picture quality while ensuring tissue specificity (15).

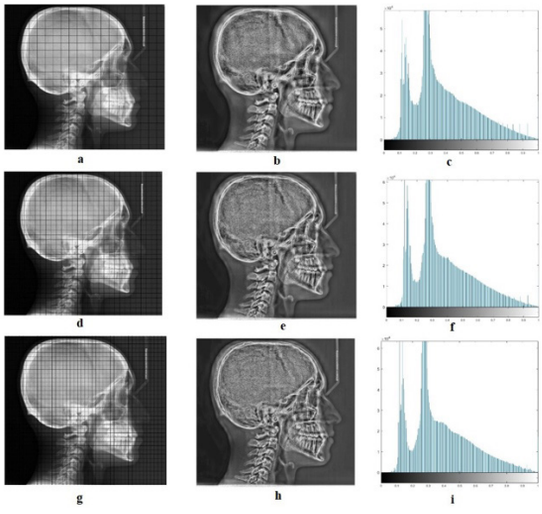

Figure 1. *The demonstration of the effects of different tile sizes in Contrast to Limited Adaptive Histogram Equalization (CLAHE) on Lateral cephalometric radiographs and histograms representing the distribution of pixel intensities.* ***a.*** *Original lateral cephalometric radiographs processed with a 20x20 tile size.* ***b.*** *The output image shows the modified contrast and clarity due to the 20x20 tile size.* ***c.*** *The image's histogram shows how the 20x20 tile size has affected the pixel intensity distribution in CLAHE.* ***d.*** *Original lateral cephalometric radiographs processed with a 30x30 tile size.* ***e.*** *The output image shows the modified contrast and clarity due to the 30x30 tile size.* ***f.*** *The image's histogram shows how the 30x30 tile size has affected the pixel intensity distribution in CLAHE.* ***g.*** *Original lateral cephalometric radiographs processed with a 40x40 tile size.* ***h.*** *The output image shows the modified contrast and clarity due to the 40x40 tile size.* ***i.*** *The image's histogram shows how the 40x40 tile size has affected the pixel intensity distribution in CLAHE.*

Figure 1 illustrates the original X-ray images processed with three different CLAHE tile sizes—20x20, 30x30, and 40x40—and their corresponding histograms. This figure succinctly demonstrates how different CLAHE tile sizes can influence the final image quality and contrast distribution. In our study, we selected a clip limit of 0.01, and the number of tiles was 20x20 for these tradeoffs using Matlab Version: R2020a 64bit (Figure 2).

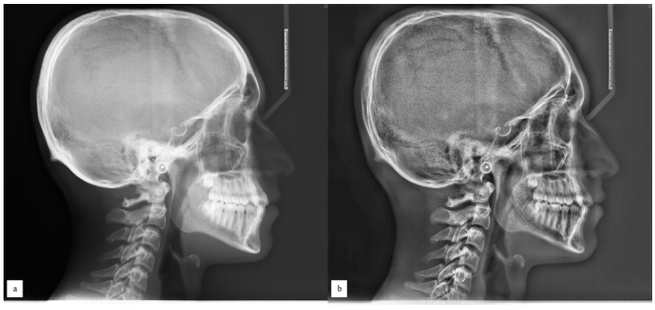

Figure 2. a: *Original lateral cephalometric radiograph,* ***b:*** *CLAHE20*20 applied lateral cephalometric radiograph*

2.2. Study Design

A fiduciary point was created in the upper-left corner of the radiograph to determine the difference between the locations of the LCR points in the original LCR and CLAHE-LCR. A macro was written using ImageJ v1.52 software (National Institutes of Health, Bethesda, MD, USA) so that the fiduciary point could be placed in a standard region in LCRs, and the location of the fiduciary point was standardized on all radiographs. Vertical and parallel planes were created from this fiduciary point, and the distances of the points at the LCRs to these planes were calculated.

CLAHE was applied to the original LCRs. The original LCR and CLAHE-LCR are shown in Figure 1 a-b, respectively. Two examiners decided on the LCRs used in this study—the soft tissue boundaries needed to be visible to both examiners without any adjustments. The brightness and contrast settings were not changed during the determination of the LCR landmark manually, so that the evaluation of the visual enhancement could be made clear. The definitions of the LCR points used in this study are listed in Table 1.

Table 1. *The definitions of the cephalometric points*

Skeletal cephalometric points	A: The deepest point of the curve of the maxilla, between the anterior nasal spine (ANS) and the dental alveolus.
	ANS (Anterior nasal spine): The tip of the anterior nasal spine.
	Ar (Articular): The intersection between posterior contour of mandible and cranial base.
	B: The deepest point of the curvature between the pogonion point and the alveolus of the mandibular incisor
	Ba (Basion): Midpoint of the anterior border of foramen magnum
	Co (Condylon): The most superior point of the mandibular condyle
	Go (Gonion): The intersection point of the lower edge of the corpus mandibularis and the posterior edge of the ramus mandibularis.
	Gn (Gnathion): Most anterior and lowest point on the mandibular symphysis
	Me (Menton): The most inferior point in the mental symphysis
	Na (Nasion): The most anterior point on frontonasal suture
	Or (Orbita): The lowest point in the inferior border of bony orbit
	PNS (Posterior nasal spine): The tip of the posterior nasal spine.
	Po (Porion): The most superior point of the external auditory meatus.
	Pog (Pogonion): The most anterior point on the chin.
Dental cephalometric points	U1IT (U1 Incisal Tip): Tip of the most prominent maxillary central incisor.
	U1RT (U1R Root Tip): Apex of the most prominent maxillary central incisor.
	L1IT (L1 Incisal Tip): Tip of the most prominent mandibular central incisor.
	L1RT (L1 Root Tip): Apex of the most prominent mandibular central incisor.
Soft tissue cephalometric points	A' (Soft tissue A): Most concave point between subnasale and the anterior point of the upper lip
	B' (Soft tissue B): Most concave point between the lower lip and the soft-tissue chin
	Gn' (Soft tissue Gnathion): Midpoint of the chin soft tissue outline between the soft tissue pogonion and soft tissue menton
	Me' (Soft tissue menton): The point where the lowest point of the soft tissue chin tip intersects with the neck plane
	Pog' (Soft Tissue pogonion): Point on the anterior curve of the soft-tissue chin
	Prn' (Pronasale): The most anterior point of nose tip
	Subnasale': Point where the nose connects to the center of the upper lip
	UpperLip': Most anterior point on the curve of the upper lip
	LowerLip': Most anterior point on the curve of the lower lip

In this study, cephalometric points were manually identified by two examiners (10 years of experience and 5 years of experience) using the AudaxCeph Advantage Cephalometric X-Ray Analysis Software Ver 4.2.0.3101 (Ljubljana, Slovenia). In addition, the same points were determined automatically using the WebCeph program, and the landmark table module was used. The working principle of the program module creates parallel and vertical planes by using the Sella point as a reference and calculating the distance of other LCR points to these planes. Thus, distance calculations were standardized by moving the sella point to the fiduciary point. Therefore, changes in the sella were not evaluated in this study.

The localization of the 27 LCR landmarks was determined by two examiners and WebCeph in both the original LCRs and the CLAHE-LCRs.

The absolute differences between the original LCRs and the CLAHE-LCRs were calculated millimeters along the x and y axes. The Euclidean distance was evaluated along the x – and y-axes by taking the square root of the sum of the squares of the changes. According to the two examiners and WebCeph, absolute differences were compared.

2.3. Measurement Error

The same orthodontist with ten years of experience repeated all measurements one month after the initial evaluation. Intraclass correlation coefficients (ICC) were utilized to assess the intra-rater agreement of landmarks in both the original and CLAHE-LCRs along the x-y axes.

2.4. Statistical Analysis

The G*Power 3.1 software (Heinrich-Heine University of Dusseldorf, Germany) was used to calculate the sample size. Post-hoc power analysis was also performed using one-way ANOVA with a 95% confidence level (1-α), d = 0.25 (medium effect size according to Cohen), three groups, and a sample size of 200. The test strength (1-β) was calculated to be 89% (18). Statistical analysis was conducted using IBM SPSS (version 21.0) software (SPSS, Chicago, IL, USA), and descriptive statistics were presented as minimum, maximum, median, mean, and standard deviation (SD). The normality of the data was assessed using histograms, normality curves, and the Kolmogorov-Smirnov test. The homogeneity of variance was checked using Levene's test.

To compare the absolute differences along the x and y axes and the Euclidean distances between the original LCRs and CLAHE-LCRs according to the examiners and WebCeph, the Kruskal Wallis test was used. Bonferroni corrections were carried out on all pairwise comparisons using Kruskal–Wallis tests. Absolute differences in the x – and y-axes within each group were evaluated using the Wilcoxon signed-rank test. In all cases, p-values of <.05 were accepted as statistically significant.

3. RESULTS

A second evaluation one month later of the same observer with ten years of experience was used to estimate the intra-class correlation coefficient (ICC). ICC greater than 0.9 indicates excellent reliability; between 0.75 and 0.9 indicates good reliability; between 0.5 and 0.75 indicates moderate reliability; and below 0.5 indicates poor reliability (19). For all cephalometric points in both the original and CLAHE-LCRs along the x-y axes, the intra-rater agreement was excellent, with an ICC value of at least 0.987.

When the accuracy values on the x-axis of the 27 landmarks were evaluated, no statistically significant difference was found among the examiners and WebCeph in A, ANS, PNS, and U1RT (p>.05). The best accuracy values along the x-axis were seen by examiner 1 in 23 of 27 landmarks, in both examiners 1 and 2 in 6 landmarks (Or, Ar, Po, Ba, Co, Go), by both examiner 1 and WebCeph in 8 landmarks (Gn, L1RT, Subnasale, Upper Lip, Lower Lip, Gn', Me', Pog') (Tables 2, 3, 4). The mean differences for the x-axis between the original LCR and CLAHE-LCR are demonstrated in Figure 3.

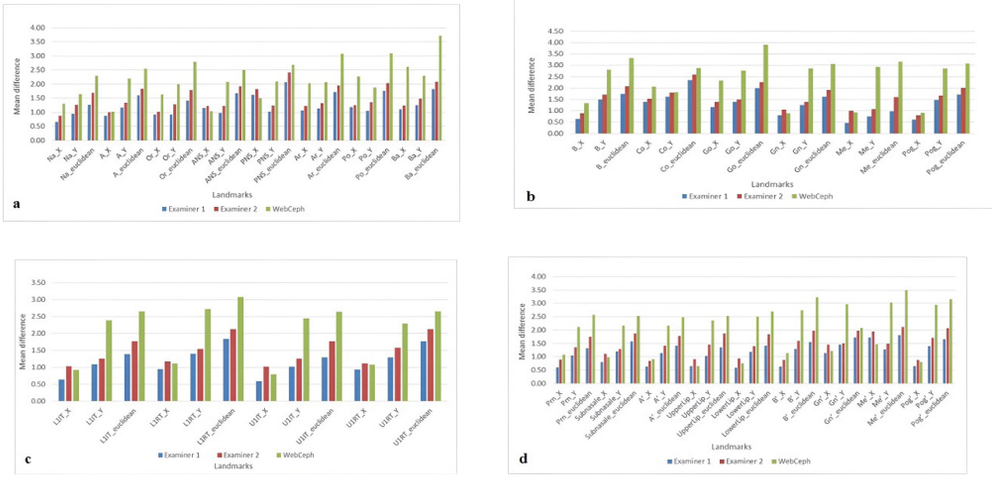

Figure 3. a-b: *Absolute difference of means along the x-y axes and Euclidean distance in skeletal landmarks,* ***c:*** *Absolute difference of means along the x-y axes and Euclidean distance in dental landmarks,* ***d:*** *Absolute difference of means along the x-y axes and Euclidean distance in soft tissue landmarks*

Table 2. *Comparison of the effects of skeletal absolute differences between the original LCR and CLAHE-LCR along the x and y axes by examiners and WebCeph*

		Examiner 1					Examiner 2					WebCeph						Post hoc comparison (mean diff.)			More accurate		
LCR Points	axis	Med.	Min.	Max.	Mean	SD	Med.	Min.	Max.	Mean	SD	Med.	Min.	Max.	Mean	SD	P	E1-E2	E1-W	E2-W	E1	E2	W
Na	X	0.54	0	2.83	0.66	0.53	0.71	0.06	3.06	0.87	0.68	1.15	0	6.95	1.3	1.19	**<.001**	**.011 (-0.21)**	**<.001 (-0.64)**	**.005 (-0.43)**	✓		
Na	Y	0.76	0.01	6.46	0.95	0.92	1.06	0	6.72	1.26	1.01	1.3	0	12.69	1.65	1.48	**<.001**	**.001 (-0.31)**	**<.001 (-0.7)**	.077 (-0.39)	✓		
A	X	0.76	0.02	4.39	0.88	0.68	0.81	0.01	4.22	1.01	0.76	0.85	0	4.53	1.01	0.79	.215	(-0.13)	(-0.13)	(0)			
A	Y	0.94	0.01	4.86	1.17	0.91	1.19	0.01	4.97	1.34	1.04	1.99	0	9.14	2.19	1.7	**<.001**	.493 (-0.17)	**<.001 (-1.02)**	**<.001 (-0.85)**	✓	✓	
Or	X	0.7	0.01	4.15	0.92	0.77	0.8	0.02	5.02	1.02	0.89	1.39	0.01	6.76	1.62	1.29	**<.001**	1 (-0.1)	**<.001 (-0.7)**	**<.001 (-0.6)**	✓	✓	
Or	Y	0.69	0	6.47	0.92	0.82	1.08	0	4.99	1.28	0.94	1.82	0.01	7.68	1.99	1.58	**<.001**	**<.001 (-0.36)**	**<.001 (-1.07)**	**<.001 (-0.71)**	✓		
ANS	X	1	0	5	1.14	0.95	1.02	0	4.55	1.22	0.99	0.79	0	5.27	1.04	0.91	.109	(-0.08)	(0.1)	(0.18)			
ANS	Y	0.82	0.01	3.53	0.98	0.78	1	0.01	4.81	1.22	0.92	1.6	0	9.5	2.07	1.77	**<.001**	**.046 (-0.24)**	**<.001 (-1.09)**	**<.001 (-0.85)**	✓		
PNS	X	1.42	0.01	6.73	1.62	1.34	1.55	0.01	6.94	1.82	1.37	1.27	0.01	7.95	1.5	1.17	.075	(-0.2)	(0.12)	(0.32)			
PNS	Y	0.9	0.01	3.78	1.03	0.76	1.07	0.01	4.64	1.24	0.93	1.8	0.01	9.48	2.09	1.62	**<.001**	.133 (-0.21)	**<.001 (-1.06)**	**<.001 (-0.85)**	✓	✓	
Ar	X	0.98	0.01	4.72	1.06	0.81	1.1	0.02	4.88	1.22	0.83	1.77	0	10.48	2.04	1.63	**<.001**	.222 (-0.16)	**<.001 (-0.98)**	**<.001 (-0.82)**	✓	✓	
Ar	Y	1.02	0.02	3.73	1.14	0.78	1.16	0	4.2	1.33	0.95	1.73	0.03	8.39	2.06	1.62	**<.001**	.349 (-0.19)	**<.001 (-0.92)**	**<.001 (-0.73)**	✓	✓	
Po	X	0.94	0	6.46	1.18	0.93	1.06	0.01	5.42	1.25	1.04	1.97	0	9.5	2.27	1.63	**<.001**	1 (-0.07)	**<.001 (-1.09)**	**<.001 (-1.02)**	✓	✓	
Po	Y	0.82	0.01	5.05	1.05	0.89	1.2	0.02	5.17	1.36	1.03	1.5	0.01	9.54	1.87	1.51	**<.001**	**.008 (-0.31)**	**<.001 (-0.82)**	**.007 (-0.51)**	✓		
Ba	X	0.87	0.01	4.37	1.1	0.89	1.04	0.02	5.25	1.23	0.9	2.28	0.02	9.62	2.62	1.99	**<.001**	.374 (-0.13)	**<.001 (-1.52)**	**<.001 (-1.39)**	✓	✓	
Ba	Y	1.04	0.01	5.24	1.25	1.02	1.27	0.02	5.99	1.48	1.11	1.86	0	9.22	2.3	1.82	**<.001**	.113 (-0.23)	**<.001 (-1.05)**	**<.001 (-0.82)**	✓	✓	
B	X	0.57	0	2.13	0.64	0.47	0.72	0	3.49	0.89	0.69	1.07	0.01	5.46	1.33	1.09	**<.001**	**.007 (-0.25)**	**<.001 (-0.69)**	**<.001 (-0.44)**	✓		
B	Y	1.28	0.05	6.22	1.49	1.13	1.51	0	6.78	1.7	1.25	2.36	0.02	11.61	2.81	2.05	**<.001**	.405 (-0.21)	**<.001 (-1.32)**	**<.001 (-1.11)**	✓	✓	
Co	X	1.08	0.04	5.43	1.38	1.07	1.35	0.04	5.98	1.52	1.15	1.78	0.03	9.66	2.05	1.55	**<.001**	.712 (-0.14)	**<.001 (-0.67)**	**.003 (-0.53)**	✓	✓	
Co	Y	1.27	0.01	6.87	1.62	1.35	1.47	0.01	7.86	1.79	1.45	1.51	0	7.42	1.82	1.46	.326	(-0.17)	(-0.2)	(-0.03)			
Go	X	0.96	0.01	4.22	1.16	0.86	1.2	0.01	4.39	1.39	0.98	1.92	0	8.94	2.32	1.8	**<.001**	.103 (-0.23)	**<.001 (-1.16)**	**<.001 (-0.93)**	✓	✓	
Go	Y	1.21	0.02	4.99	1.39	1.06	1.25	0.01	5.37	1.5	1.1	2.39	0.01	10.36	2.77	2.15	**<.001**	1 (-0.11)	**<.001 (-1.38)**	**<.001 (-1.27)**	✓	✓	
Gn	X	0.67	0.01	4.91	0.81	0.68	0.91	0	3.97	1.05	0.75	0.75	0	4.78	0.89	0.74	**.002**	**.002 (-0.24)**	.896 (-0.08)	**.048 (0.16)**	✓		✓
Gn	Y	1.01	0	5.23	1.24	1	1.12	0.01	5.09	1.38	1.14	2.55	0	12.78	2.86	2.16	**<.001**	1 (-0.14)	**<.001 (-1.62)**	**<.001 (-1.48)**	✓	✓	
Me	X	0.35	0	2.67	0.47	0.43	0.84	0.01	3.36	1	0.67	0.78	0.01	4.98	0.93	0.75	**<.001**	**<.001 (-0.53)**	**<.001 (-0.46)**	.178 (0.07)	✓		
Me	Y	0.51	0	5.11	0.75	0.86	0.83	0.01	5.41	1.07	0.95	2.59	0	12.63	2.93	2.23	**<.001**	**<.001 (-0.32)**	**<.001 (-2.18)**	**<.001 (-1.86)**	✓		
Pog	X	0.46	0.02	2.59	0.6	0.5	0.68	0	2.53	0.81	0.59	0.78	0.01	4.45	0.91	0.72	**<.001**	**.001 (-0.21)**	**<.001 (-0.31)**	.581 (-0.1)	✓		
Pog	Y	1.14	0.01	5.65	1.47	1.16	1.41	0.01	5.5	1.67	1.27	2.49	0.02	12.79	2.85	2.12	**<.001**	.488 (-0.2)	**<.001 (-1.38)**	**<.001 (-1.18)**	✓	✓	

[*] *Significant results according to Kruskal Wallis test, Bonferroni corrections were carried out on all pair-wise comparisons of Kruskal–Wallis tests. (p<.05)*

LCR; lateral cephalometric radiograph, Med; median, Min; minimum, Max; maximum, SD; standard deviation, E; Examiner, W;WebCeph, Clahe;Contrast-Limited Adaptive Histogram Equalization

Table 3. *Comparison of the effects of dental absolute differences between the original LCR and CLAHE-LCR along the x and y axes by examiners and WebCeph*

		Examiner 1					Examiner 2					WebCeph						Post hoc comparison (mean diff.)			More accurate		
LCR Points	axis	Med.	Min.	Max.	Mean	SD	Med.	Min.	Max.	Mean	SD	Med.	Min.	Max.	Mean	SD	P	E1-E2	E1-W	E2-W	E1	E2	W
L1IT	X	0.54	0.01	2.1	0.64	0.49	0.88	0.01	3.51	1.03	0.66	0.85	0.01	3.91	0.93	0.7	**<.001**	**<.001 (-0.39)**	**<.001 (-0.29)**	.127 (0.1)	✓		
L1IT	Y	0.88	0	4.18	1.09	0.87	1.11	0.03	4.25	1.26	0.92	2.07	0	9.74	2.39	1.79	**<.001**	.246 (-0.17)	**<.001 (-1.3)**	**<.001 (-1.13)**	✓	✓	
L1RT	X	0.74	0.01	3.77	0.95	0.75	1.06	0.01	5	1.17	0.86	0.94	0.01	5.16	1.11	0.85	**.018**	**.019 (-0.22)**	.124 (-0.16)	1 (0.06)	✓		✓
L1RT	Y	1.13	0.01	5.33	1.4	1.08	1.45	0.01	6.12	1.54	1.12	2.32	0.04	11.99	2.73	2.03	**<.001**	.588 (-0.14)	**<.001 (-1.33)**	**<.001 (-1.19)**	✓	✓	
U1IT	X	0.52	0	2.69	0.59	0.49	0.88	0	3.57	1.02	0.73	0.7	0.01	3.74	0.79	0.62	**<.001**	**<.001 (-0.43)**	**.005 (-0.2)**	**.005 (0.23)**	✓		
U1IT	Y	0.81	0	4.04	1.03	0.82	1.05	0	4.37	1.26	0.95	2.22	0.01	10.33	2.45	1.84	**<.001**	.092 (-0.23)	**<.001 (-1.42)**	**<.001 (-1.19)**	✓	✓	
U1RT	X	0.77	0	3.46	0.94	0.76	0.97	0	4.99	1.12	0.86	0.86	0	5.28	1.07	0.91	.111	(-0.18)	(-0.13)	(0.05)			
U1RT	Y	1.09	0	4.16	1.3	0.99	1.26	0.01	5.6	1.58	1.24	2.07	0.02	7.99	2.29	1.66	**<.001**	.214 (-0.28)	**<.001 (-0.99)**	**<.001 (-0.71)**	✓	✓	

* *Significant results according to Kruskal Wallis test, Bonferroni corrections were carried out on all pair-wise comparisons of Kruskal–Wallis tests. (p<.05)*

LCR; lateral cephalometric radiograph, Med; median, Min; minimum, Max; maximum, SD; standard deviation, E; Examiner, W;WebCeph, Clahe;Contrast-Limited Adaptive Histogram Equalization

Table 4. *Comparison of the effects of soft tissue absolute differences between the original LCR and the CLAHE-LCR along the x and y axes by examiners and WebCeph*

		Examiner 1					Examiner 2					WebCeph						Post hoc comparison (mean diff.)			More accurate		
LCR Points	axis	Med.	Min.	Max.	Mean	SD	Med.	Min.	Max.	Mean	SD	Med.	Min.	Max.	Mean	SD	P	E1-E2	E1-W	E2-W	E1	E2	W
Prn	X	0.46	0	2.44	0.6	0.52	0.69	0	2.93	0.88	0.65	0.93	0	6.2	1.07	0.92	**<.001**	**<.001 (-0.28)**	**<.001 (-0.47)**	.535 (-0.19)	✓		
Prn	Y	0.76	0	4.45	1.04	0.91	1.16	0	5.29	1.34	1.03	1.7	0.01	8.53	2.11	1.65	**<.001**	**.007 (-0.3)**	**<.001 (-1.07)**	**<.001 (-0.77)**	✓		
Subnasale	X	0.69	0.01	2.74	0.8	0.6	0.93	0.01	4.47	1.11	0.84	0.89	0	3.47	0.98	0.71	**.001**	**.001 (-0.31)**	.52 (-0.18)	.645 (0.13)	✓		✓
Subnasale	Y	0.98	0.02	5.39	1.2	0.97	1.08	0	5.63	1.29	1.04	1.84	0	9.6	2.16	1.68	**<.001**	1 (-0.1)	**<.001 (-0.96)**	**<.001 (-0.87)**	✓	✓	
A’	X	0.55	0	2.05	0.63	0.46	0.76	0.01	2.75	0.85	0.61	0.82	0.01	3.06	0.9	0.67	**<.001**	**.002 (-0.22)**	**<.001 (-0.27)**	1 (-0.05)	✓		
A’	Y	0.87	0.01	4.96	1.14	0.98	1.25	0.01	4.91	1.41	1.08	2.03	0	9.57	2.16	1.66	**<.001**	**.042 (-0.27)**	**<.001 (-1.02)**	**<.001 (-0.75)**	✓		
UpperLip	X	0.49	0	3.32	0.65	0.59	0.85	0	3.47	0.91	0.62	0.51	0	4.41	0.64	0.6	**<.001**	**<.001 (-0.26)**	1 (0.01)	**<.001 (0.27)**	✓		✓
UpperLip	Y	0.7	0	4.82	1.03	0.92	1.25	0	5.31	1.45	1.16	2.05	0	10.14	2.35	1.81	**<.001**	**.001 (-0.42)**	**<.001 (-1.32)**	**<.001 (-0.9)**	✓		
LowerLip	X	0.52	0	2.22	0.59	0.46	0.81	0	3.16	0.94	0.7	0.57	0	3.43	0.75	0.66	**<.001**	**<.001 (-0.35)**	.087 (-0.16)	**<.001 (0.19)**	✓		✓
LowerLip	Y	0.94	0.01	4.83	1.18	0.93	1.23	0.01	4.46	1.39	1	2.1	0	11.09	2.5	1.96	**<.001**	.144 (-0.21)	**<.001 (-1.32)**	**<.001 (-1.11)**	✓		
B’	X	0.54	0	2.22	0.63	0.46	0.75	0	3.03	0.87	0.63	0.85	0	11.27	1.13	1.17	**<.001**	**.001 (-0.24)**	**<.001 (-0.5)**	.389 (-0.26)	✓		
B’	Y	0.97	0.01	6.21	1.29	1.11	1.39	0	6.12	1.59	1.21	2.34	0	12.81	2.74	2.07	**<.001**	.055 (-0.3)	**<.001 (-1.45)**	**<.001 (-1.15)**	✓	✓	
Gn’	X	0.99	0.01	5.1	1.14	0.93	1.26	0.01	6.47	1.46	1.11	1.01	0	9.95	1.2	1.07	**.006**	**.007 (-0.32)**	1 (-0.06)	**.044 (0.26)**	✓		✓
Gn’	Y	1.17	0.02	6.5	1.45	1.14	1.19	0.01	6.46	1.5	1.27	2.52	0.03	13.55	2.96	2.31	**<.001**	1 (-0.05)	**<.001 (-1.51)**	**<.001 (-1.46)**	✓	✓	
Me’	X	1.38	0	6.51	1.72	1.38	1.68	0.01	8.34	1.95	1.43	1.27	0.01	6.54	1.47	1.17	**.002**	.193 (-0.23)	.304 (0.25)	**.001 (0.48)**	✓		✓
Me’	Y	0.93	0.02	4.77	1.28	1.05	1.25	0.02	5.18	1.48	1.1	2.65	0	12.74	3.03	2.3	**<.001**	.192 (-0.2)	**<.001 (-1.75)**	**<.001 (-1.55)**	✓	✓	
Pog’	X	0.54	0	3.22	0.64	0.52	0.78	0	3.18	0.87	0.64	0.66	0.01	10.22	0.79	0.9	**.001**	**<.001 (-0.23)**	.23 (-0.15)	.131 (0.08)	✓		✓
Pog’	Y	1.14	0	5.07	1.4	1.09	1.52	0	5.49	1.7	1.21	2.5	0.01	13.73	2.94	2.2	**<.001**	.074 (-0.3)	**<.001 (-1.54)**	**<.001 (-1.24)**	✓	✓	

* *Significant results according to Kruskal Wallis test, Bonferroni corrections were carried out on all pair-wise comparisons of Kruskal–Wallis tests. (p<.05)*

LCR; lateral cephalometric radiograph, Med; median, Min; minimum, Max; maximum, SD; standard deviation, E; Examiner, W;WebCeph, Clahe;Contrast-Limited Adaptive Histogram Equalization

*Kruskal Wallis test, Bonferroni corrections were carried out on all pair-wise comparisons of Kruskal–Wallis tests. *significance on p < .05 scale*

Table 5. *Comparison of absolute differences between original LCRs and CLAHE LCRs along the x and y axes within examiners and WebCeph themselves*

LCR Points	Examiner 1		Examiner 2		WebCeph	
	mean diff. (x-y)	p	mean diff. (x-y)	p	mean diff. (x-y)	p
Na	-0.29	**<.001**	-0.39	**<.001**	-0.35	**.001**
A	-0.29	**<.001**	-0.33	.1	-1.18	**<.001**
Or	0	.972	-0.26	**.003**	-0.37	**.004**
ANS	0.16	.151	0	.817	-1.03	**<.001**
PNS	0.59	**<.001**	0.58	**<.001**	-0.59	**<.001**
Ar	-0.08	.212	-0.11	.109	-0.02	.464
Po	0.13	.119	-0.11	.188	0.4	**<.001**
Ba	-0.15	.77	-0.25	**.006**	0.32	.25
B	-0.85	**<.001**	-0.81	**<.001**	-1.48	**<.001**
Co	-0.24	.54	-0.27	**.045**	0.23	**.008**
Go	-0.23	**.014**	-0.11	.395	-0.45	**.007**
Gn	-0.43	**<.001**	-0.33	**.001**	-1.97	**<.001**
Me	-0.28	**<.001**	-0.07	.541	-2	**<.001**
Pog	-0.87	**<.001**	-0.86	**<.001**	-1.94	**<.001**
L1IT	-0.45	**<.001**	-0.23	**.009**	-1.46	**<.001**
L1RT	-0.45	**<.001**	-0.37	**.001**	-1.62	**<.001**
U1IT	-0.44	**<.001**	-0.24	**.003**	-1.66	**<.001**
U1RT	-0.36	**<.001**	-0.46	**<.001**	-1.22	**<.001**
Prn	-0.44	**<.001**	-0.46	**<.001**	-1.04	**<.001**
Subnasale	-0.4	**<.001**	-0.18	**.038**	-1.18	**<.001**
A’	-0.51	**<.001**	-0.56	**<.001**	-1.26	**<.001**
UpperLip	-0.38	**<.001**	-0.54	**<.001**	-1.71	**<.001**
LowerLip	-0.59	**<.001**	-0.45	**<.001**	-1.75	**<.001**
B’	-0.66	**<.001**	-0.72	**<.001**	-1.61	**<.001**
Gn’	-0.31	**.002**	-0.04	.928	-1.76	**<.001**
Me’	0.44	**<.001**	0.47	**.001**	-1.56	**<.001**
Pog’	-0.76	**<.001**	-0.83	**<.001**	-2.15	**<.001**

** Significant results according to Wilcoxon Signed Rank Test (p<.05)*
LCR; lateral cephalometric radiograph, E; Examiner, W;WebcephX, Clahe;Contrast-Limited Adaptive Histogram Equalization
*Wilcoxon Signed Rank Test. *significance on p < .05 scale*

When the accuracy values in the y-axis of 27 landmarks were evaluated, no statistically significant difference was found between the examiners and WebCeph in Co (p>.05). The best accuracy values along the y-axis were seen by Examiner 1 in 26 of the 27 landmarks, while in both examiners 1 and 2 in 17 landmarks. The worst accuracy values were obtained for all landmarks in WebCeph (Tables 2-4). The mean differences for the y-axis between the original LCR and CLAHE-LCR are demonstrated in Figure 3.

When the differences in the x and y axes were compared with each other, there was no statistically significant difference in Or, ANS, Ar, Po, Ba, and Co by Examiner 1, in A, ANS, Ar, Po, Go, Me by Examiner 2, and Ba in WebCeph (p>.05). Statistically, differences between examiners and WebCeph were generally more pronounced on the y-axis (p<.05). The exceptions were PNS and Me’ for examiners and Po and Co for WebCeph (p<.05) (Table 5). The mean differences in the x – and y – axes according to image methods by examiners and WebCeph are demonstrated in Figure 4.

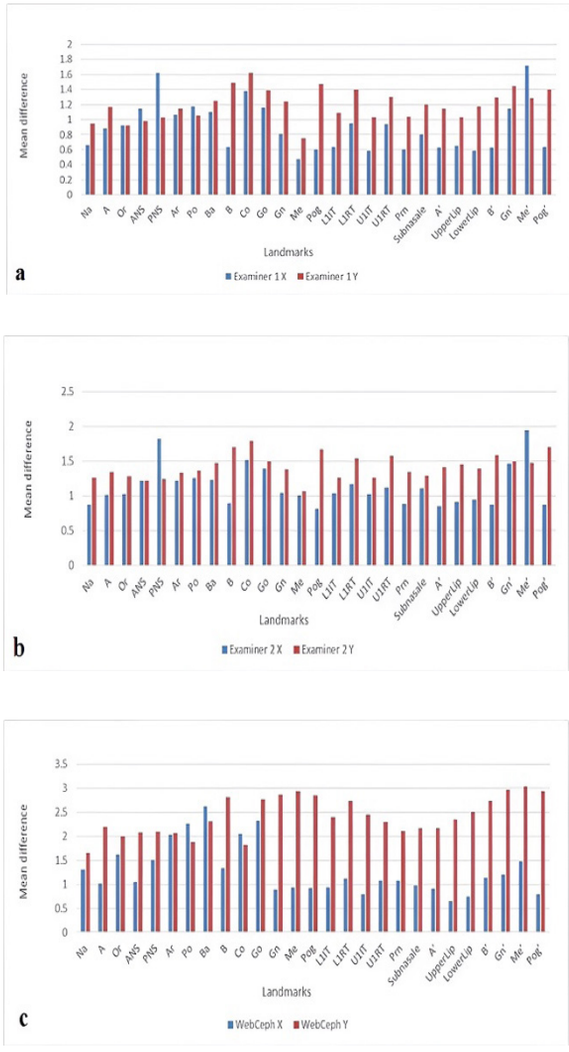

Figure 4. *a: Absolute difference of means along the x-y axes by Examiner 1, b: Absolute difference of means along the x-y axes by Examiner 2, c: Absolute difference of means along the x-y axes in WebCeph*

When the accuracy values in the Euclidean distance of 27 landmarks were evaluated, significant differences were found between the examiners and WebCeph in all measurements. The best accuracy values were seen by Examiner 1 for all landmarks, and by both examiners 1 and 2 for five landmarks. The worst accuracy values were obtained for all landmarks using WebCeph (Table 6). The mean differences in the Euclidean distance between the original LCR and CLAHE-LCR are shown in Figure 3.

The differences between the original LCR and the CLAHE-LCR are shown in supplementary material for both two examiners and WebCeph.

Table 6. *Comparison of the effects of euclidean differences between the original LCR and the CLAHE-LCR by examiners and WebCeph*

		Examiner 1					Examiner 2					WebCeph						Post hoc comparison		More accurate		
LCR Points		Med.	Min.	Max.	Mean	SD	Med.	Min.	Max.	Mean	SD	Med.	Min.	Max.	Mean	SD	P	E1-E2	E1-W	E2-W	E1	E2	W
Na	euclidean	1.07	0.04	6.54	1.27	0.92	1.5	0.26	6.84	1.69	0.99	1.95	0.08	12.71	2.29	1.66	**<.001**	**<.001 (-0.42)**	**<.001 (-1.02)**	**.002 (-0.6)**	✓		
A	euclidean	1.39	0.16	5.04	1.6	0.94	1.63	0.14	5.02	1.83	1.04	2.22	0.16	9.67	2.54	1.7	**<.001**	.63 (-0.23)	**<.001 (-0.94)**	**<.001 (-0.71)**	✓	✓	
Or	euclidean	1.18	0.09	7.69	1.42	0.98	1.59	0.08	6.92	1.79	1.07	2.5	0.15	8.3	2.79	1.72	**<.001**	**.001 (-0.37)**	**<.001 (-1.37)**	**<.001 (-1)**	✓		
ANS	euclidean	1.55	0.07	5.12	1.67	0.99	1.73	0.08	5.35	1.91	1.07	2.16	0.12	9.5	2.5	1.76	**<.001**	.66 (-0.24)	**<.001 (-0.83)**	**.017 (-0.59)**	✓	✓	
PNS	euclidean	1.9	0.12	6.78	2.07	1.32	2.27	0.14	7.01	2.41	1.34	2.42	0.21	12.37	2.69	1.83	**.001**	**.014 (-0.34)**	**.001 (-0.62)**	1.00 (-0.28)	✓		
Ar	euclidean	1.61	0.14	4.73	1.71	0.88	1.85	0.17	4.88	1.95	1.02	2.82	0.11	11.7	3.07	2.05	**<.001**	.111 (-0.24)	**<.001 (-1.36)**	**<.001 (-1.12)**	✓	✓	
Po	euclidean	1.58	0.12	6.49	1.76	1.02	1.78	0.09	5.72	2.03	1.19	2.6	0.25	11.75	3.09	2.01	**<.001**	.114 (-0.27)	**<.001 (-1.33)**	**<.001 (-1.06)**	✓	✓	
Ba	euclidean	1.57	0.04	5.38	1.82	1.14	1.81	0.31	6.36	2.08	1.19	3.49	0.14	13.32	3.72	2.36	**<.001**	.14 (-0.26)	**<.001 (-1.9)**	**<.001 (-1.64)**	✓	✓	
B	euclidean	1.56	0.15	6.24	1.73	1.06	1.91	0.09	6.79	2.08	1.17	3.01	0.3	12.03	3.31	2.02	**<.001**	**.011 (-0.35)**	**<.001 (-1.58)**	**<.001 (-1.23)**	✓		
Co	euclidean	2.1	0.2	7.63	2.34	1.43	2.45	0.15	8.1	2.6	1.47	2.39	0.09	9.97	2.87	1.95	**.036**	.164 (-0.26)	**.044 (-0.53)**	1 (-0.27)	✓	✓	
Go	euclidean	1.81	0.13	5.07	1.98	1.09	2.17	0.2	5.45	2.25	1.13	3.44	0.23	11.8	3.9	2.38	**<.001**	**.08 (-0.27)**	**<.001 (-1.92)**	**<.001 (-1.65)**	✓		
Gn	euclidean	1.4	0.13	5.73	1.61	1.03	1.67	0.12	5.48	1.91	1.11	2.76	0.06	13.64	3.05	2.21	**<.001**	**.028 (-0.3)**	**<.001 (-1.44)**	**<.001 (-1.14)**	✓		
Me	euclidean	0.79	0.01	5.17	0.98	0.85	1.4	0.11	5.56	1.6	0.96	2.76	0.11	13.58	3.16	2.25	**<.001**	**<.001 (-0.62)**	**<.001 (-2.18)**	**<.001 (-1.56)**	✓		
Pog	euclidean	1.5	0.06	5.71	1.71	1.09	1.79	0.28	5.92	2.01	1.16	2.61	0.08	13.54	3.08	2.13	**<.001**	**.03 (-0.3)**	**<.001 (-1.37)**	**<.001 (-1.07)**	✓		
L1IT	euclidean	1.25	0.05	4.3	1.38	0.82	1.7	0.03	4.57	1.77	0.88	2.31	0.07	10.5	2.65	1.8	**<.001**	**<.001 (-0.39)**	**<.001 (-1.27)**	**<.001 (-0.88)**	✓		
L1RT	euclidean	1.55	0.19	5.48	1.84	1.09	2	0.06	6.79	2.12	1.11	2.68	0.28	13.05	3.08	2	**<.001**	**.042 (-0.28)**	**<.001 (-1.24)**	**<.001 (-0.96)**	✓		
U1IT	euclidean	1.17	0.02	4.13	1.3	0.79	1.68	0.02	4.79	1.76	0.96	2.3	0.05	10.99	2.64	1.85	**<.001**	**<.001 (-0.46)**	**<.001 (-1.34)**	**<.001 (-0.88)**	✓		
U1RT	euclidean	1.66	0.08	5.18	1.77	1	1.98	0.12	6.39	2.12	1.22	2.26	0.25	8.82	2.65	1.72	**<.001**	**.016 (-0.35)**	**<.001 (-0.88)**	**.03 (-0.53)**	✓		
Prn	euclidean	1.08	0.07	5.03	1.32	0.9	1.57	0.1	5.77	1.74	1.02	2.22	0.13	9.56	2.57	1.6	**<.001**	**<.001 (-0.42)**	**<.001 (-1.25)**	**<.001 (-0.83)**	✓		
Subnasale	euclidean	1.43	0.25	5.41	1.58	0.94	1.76	0.07	5.82	1.87	1.08	2.26	0.2	10	2.52	1.6	**<.001**	**.022 (-0.29)**	**<.001 (-0.94)**	**<.001 (-0.65)**	✓		
A’	euclidean	1.23	0.13	5.33	1.4	0.94	1.68	0.09	5.01	1.78	1.03	2.36	0.14	10.01	2.48	1.59	**<.001**	**<.001 (-0.38)**	**<.001 (-1.08)**	**<.001 (-0.7)**	✓		
UpperLip	euclidean	1.16	0.07	4.85	1.36	0.91	1.69	0.1	5.38	1.86	1.09	2.16	0.1	10.71	2.52	1.81	**<.001**	**<.001 (-0.5)**	**<.001 (-1.16)**	**.019 (-0.66)**	✓		
LowerLip	euclidean	1.29	0.03	4.91	1.42	0.9	1.83	0.06	4.47	1.84	0.96	2.21	0.12	11.61	2.7	1.96	**<.001**	**<.001 (-0.42)**	**<.001 (-1.28)**	**.004 (-0.86)**	✓		
B’	euclidean	1.26	0.15	6.47	1.55	1.04	1.78	0.06	6.14	1.97	1.12	2.88	0.48	13.1	3.22	2.02	**<.001**	**<.001 (-0.42)**	**<.001 (-1.67)**	**<.001 (-1.25)**	✓		
Gn’	euclidean	1.63	0.14	5.34	1.72	0.92	1.86	0.2	6.77	1.97	1.09	1.78	0.15	10.12	2.09	1.38	**.024**	.064 (-0.25)	**.046 (-0.37)**	1 (-0.12)	✓	✓	
Me’	euclidean	1.66	0.1	5.37	1.8	1.08	1.94	0.28	5.95	2.11	1.14	3.24	0	14.84	3.49	2.42	**<.001**	**.033 (-0.31)**	**<.001 (-1.69)**	**<.001 (-1.38)**	✓		
Pog’	euclidean	1.37	0.13	5.13	1.66	1.04	1.85	0.08	5.5	2.06	1.12	2.64	0.1	14.24	3.15	2.24	**<.001**	**.002 (-0.4)**	**<.001 (-1.49)**	**<.001 (-1.09)**	✓		

** Significant results according to Kruskal Wallis test, Bonferroni corrections were carried out on all pair-wise comparisons of Kruskal–Wallis tests. (p<.05)*

LCR; lateral cephalometric radiograph, Med; median, Min; minimum, Max; maximum, SD; standard deviation, E; Examiner, W;WebCeph, Clahe;Contrast-Limited Adaptive Histogram Equalization

4. DISCUSSION

"Accuracy" throughout the manuscript refers to evaluating a cephalometric landmark by comparison of the differences (x, y-axes, and Euclidean distances) between the original LCRs and CLAHE LCRs. When evaluating original LCRs and CLAHE LCRs from the same individual, consistent results in LCR point determination, regardless of visual characteristics, mean high accuracy.

The majority of the research in the literature compared the efficiency of AI-based algorithms to expert point localization as ground truth (7,14). Rather than ground truth-based evaluation, the primary purpose of our study was to compare the responses of both examiners and the AI-based software in inconsistencies between original and CLAHE LCRs.

To our knowledge, no previous study has investigated the efficacy of CLAHE in identifying cephalometric landmarks in WebCeph and human examiners. The efficacy of CLAHE was tested on 27 LCR landmarks. The first null hypothesis, which stated that there would be no difference in landmark identification accuracy between WebCeph and human examiners based on the method used, was not rejected. The second null hypothesis, which stated that there would be no difference in accuracy in identifying LCR landmarks between the x – and y – axes based on comparisons made by both examiners and WebCeph itself, was also not rejected.

Interpreting radiographic images requires radiological information, pattern recognition, and image quality. Improving landmark determination accuracy improves image quality (20,21). Computerized digital radiography systems can adjust image contrast and brightness. Edge enhancement is one of the most popular methods since it selectively increases image edges, making identifying anatomical landmarks easier. Based on the particular requirements of the radiographic examination, these approaches can improve image quality in darker or lighter areas or the overall radiographic image. These image enhancement methods can improve landmark identification accuracy and consistency, contributing to more accurate diagnoses (22).

Studies in the literature have evaluated the effects of image enhancement on landmark detection errors based on manual tracing in standard LCRs and digital LCRs along the x-y axes (23-25). In digital radiography, sharpness and contrast changes can enhance the image. Thus, anatomical landmarks can be determined more easily (10,26). The differences between the examiners were less than 1 mm in all measurements of differences between the original LCR and the CLAHE-LCR. Although there were statistically significant differences in some landmarks between the examiners, it may not be a clinically important difference. From a clinical point of view, 1 mm is an acceptable error limit for identifying cephalometric points regarding the examiners (27).

Eppley and Sadove (10) reported that standard LCRs and digitally enhanced LCRs showed comparable accuracy in identifying bone landmarks, but digital enhancement was superior in identifying soft tissue. Nikneshan et al. (28) reported that the original LCRs provided better reliability at Co, Or, and Pog, while the emboss image enhancement LCRs provided better reliability at A, ANS, B, Ba, Me', L1IT. It was stated that the effect of the embossing method on the reliability of landmarks was greater in the x plane than in the y plane.

In this study, the CLAHE method changed the y-axis more than the x-axis in two examiners and WebCeph. The x-axis results were more consistent for examiners (except PNS, Me') and WebCeph (except Po, Co).

The literature mentions acceptable mean errors for automatic landmark detection in orthodontic practice and research. For the x coordinate, 0.59 mm of mean error is acceptable, and for the y coordinate, 0.56 mm. Although the Euclidean mean error value of ±0.81 mm is recommended, it is not commonly used. A successful difference in automatic landmark detection is generally considered to have a difference of ≤2 mm from a human operator and an acceptable difference of ≤4 mm. (29-34). In this study, the CLAHE caused over 0.59 mm error on the x-axis and 0.56 mm on the y-axis in all measurements for both examiners and AI. The mean Euclidean distances were greater than 2 mm in Co, PNS by Examiner 1, Po, Ba, Co, Go, Pog, U1RT, Me', Pog by Examiner 2, and in all measurements by WebCeph. Both examiners and WebCeph had Euclidean distance differences of less than 4 mm. This study showed that WebCeph had higher Euclidean distance differences than examiners. This indicated that WebCeph performed less accurately than trained orthodontists manually.

Hwang et al. (33) reported that YOLOv3 performed better than human examiners in repeated measurements in original LCRs. Our study compared the differences between the original LCR and CLAHE-LCR. For almost all LCR landmarks, WebCeph's differences were greater than the differences of examiners.

CLAHE has been used in dentistry to detect caries in radiographs, identify gingivitis in photos, pulp capping treatment, endodontic therapy, and improve radiographic image quality (16,35-39). In orthodontics, Nishimoto et al. (40) found no significant difference between manual and AI-assisted LCR point determination in angular and linear measurements using CLAHE. The gonion had the highest landmark error in Nishimoto's and our study (Examiner 2 and WebCeph). However, angular or linear measurements were not examined in our study.

The highest Euclidean errors in skeletal landmarks were Co and PNS in examiners and Go and Ba in WebCeph. Anatomical superpositions are common in the posterior LCR region, where these landmarks are. The Co and Ba landmarks overlap complex anatomical structures, making identification difficult. The auricular structures of X-ray machines may cover the area, making identification challenging (23,41). Ba was also the second-least accurate landmark in WebCeph. Blurring the image led by the CLAHE method and overlapping adjacent or bilateral structures have made it challenging to identify Ba.

The PNS, the posterior limit of the hard palate, can be difficult to locate on radiographic images because, as the hard palate extends towards the back, it becomes less visible on the image because of the more transparent soft palate (23). The CLAHE technique reduced image contrast and sharpness, making it difficult for examiners to find the PNS border horizontally rather than vertically.

Go is on a curved structure connecting the corpus and mandibular ramus. Mandibular shape or head position variations overlap structures, making locating difficult (23,41,42). Identifying the gonion in CLAHE-LCRs is more challenging because the image-processing technique could grey out surrounding areas, especially in double-contoured regions.

WebCeph had higher dental Euclidean mean errors than the examiners, and Examiner 1 had the lowest. The highest errors by the examiners belonged to U1RT and L1RT, while the highest for WebCeph belonged to L1RT. On WebCeph, however, the Euclidean errors of the other dental landmarks (except L1RT) were close. The reason for this can be seen in L1RT rather than U1RT may be that the bone in the maxilla has a porous structure, while the mandible has a compact structure, and this situation is more pronounced in the mandible due to the decreased sharpness and increased greyness in CLAHE.

The CLAHE method enhanced the visibility of soft tissue. WebCeph had higher Euclidean mean soft tissue landmark differences than examiners. Examiner 1 had the lowest soft tissue landmark error. The highest soft tissue landmark errors were Me' and Gn' for examiner 1, Me' and Pog' for examiner 2, and Me' and Pog' for WebCeph. Gn' and Pog' changed significantly on the y-axis for both examiners and WebCeph, while Me' changed significantly on the x-axis.

Ha et al. (43) used a YOLOv3-based convolutional neural network model to diagnose mesiodens and found that CLAHE images had lower accuracy, sensitivity, and specificity internally and externally. Image enhancement may not improve AI-based application accuracy.

Menezes et al. (44) reported that their AI-based program is excellent for cephalometric analysis. However, low brightness and strong contrast affect program landmark reproducibility and require human supervision to be clinically reliable. They suggested extra machine learning rounds for accurate landmark localization in images with variable brightness and contrast, especially for bilateral landmarks like Or and Po. Our findings confirmed the need for manual adjustment, similar to them. The differences between the original LCR and CLAHE-LCR were lower in examiners than in WebCeph.

The main limitation of this study is that only two investigators evaluated reliability, and it was a single-center study. Another limitation is that the study sample was selected only from individuals with permanent dentition. No evaluation was performed in individuals with mixed dentition or orthodontic appliances in the mouth.

5. CONCLUSION

The use of CLAHE in WebCeph requires more adjustments to identify landmarks accurately compared to the manual system. Therefore, further research is required to enhance the performance of the CLAHE method in automated systems. In most measurements, the mean differences between the original LCR and CLAHE-LCR were more significant along the y-axis than the x-axis. For this reason, the y-axis should be evaluated more carefully when evaluating the landmark position in CLAHE-LCR.

Acknowledgement: *Thank you for supporting the participants in this study.*
Funding: *The author(s) received no financial support for the research.*
Conflicts of interest: *The authors declare that they have no conflict of interest.*
Ethics Committee Approval: *This study was approved by Ethics Committee of Recep Tayyip Erdogan University Medical Faculty, (approval date 30.09.2021 and number 2021/168)*
Peer-review: *Externally peer-reviewed.*
Author Contributions:
Research idea: MG
Design of the study: MG, ÇST
Acquisition of data for the study: MG, ŞG
Analysis of data for the study: MG, ÇST
Interpretation of data for the study: MG, ÇST, ŞG
Drafting the manuscript: MG, ÇST
Revising it critically for important intellectual content: MG, ÇST, ŞG
Final approval of the version to be published: MG, ÇST, ŞG

REFERENCES

[1] Devereux L, Moles D, Cunningham SJ, McKnight M. How important are lateral cephalometric radiographs in orthodontic treatment planning?. Am J Orthod Dentofacial Orthop. 2011;139(2):e175-e181. DOI: 10.1016/j.ajodo.2010.09.021.

[2] Junaid N, Khan N, Ahmed N, Abbasi MS, Das G, Maqsood A, Ahmed AR, Marya A, Alam MK, Heboyan A. Development, application, and performance of artificial intelligence in cephalometric landmark identification and diagnosis: A systematic review. Healthcare (Basel). 2022;10(12):2454. DOI: 10.3390/healthcare10122454.

[3] Wong SH, Al-Hasani H, Alam Z, Alam A. Artificial intelligence in radiology: How will we be affected?. Eur Radiol. 2019;29(1):141-143. DOI: 10.1007/s00330.018.5644-3.

[4] Ahmed N, Abbasi MS, Zuberi F, Qamar W, Halim MSB, Maqsood A, Alam MK. Artificial intelligence techniques: Analysis, application, and outcome in dentistry-a systematic review. Biomed Res Int. 2021;2021:1-15. DOI: 10.1155/2021/9751564.

[5] Nguyen TT, Larrivée N, Lee A, Bilaniuk O, Durand R. Use of artificial intelligence in dentistry: Current clinical trends and research advances. J Can Dent Assoc. 2021;87:l7.

[6] Kiełczykowski M, Kamiński K, Perkowski K, Zadurska M, Czochrowska E. Application of artificial intelligence (ai) in a cephalometric analysis: A narrative review. Diagnostics (Basel). 2023;13(16):2640. DOI: 10.3390/diagnostics13162640.

[7] Kim H, Shim E, Park J, Kim YJ, Lee U, Kim Y. Web-based fully automated cephalometric analysis by deep learning. Comput Methods Programs Biomed. 2020;194:105513. DOI: 10.1016/j.cmpb.2020.105513.

[8] Houston WJ. The analysis of errors in orthodontic measurements. Am J Orthod. 1983;83(5):382-390. DOI: 10.1016/0002-9416(83)90322-6.

[9] Midtgård J, Björk G, Linder-Aronson ST. Reproducibility of cephalometric landmarks and errors of measurements of cephalometric cranial distances. Angle Orthod. 1974;44(1):56-61. DOI: 10.1043/0003-3219(1974)044<0056:ROCLAE>2.0.CO;2.

[10] Eppley BL, Sadove AM. Computerized digital enhancement in craniofacial cephalometric radiography. J Oral Maxillofac Surg. 1991;49(10):1038-1043. DOI: 10.1016/0278-2391(91)90133-7.

[11] Ismail WZ, Sim KS. Contrast enhancement dynamic histogram equalization for medical image processing application. Int J Imaging Syst Technol. 2011;21(3):280-289. DOI: 10.1002/ima.20295.

[12] Zuiderveld K. Contrast limited adaptive histogram equalization. In: Heckbert PS, editor. Graphics Gems IV. Cambridge, MA: Academic Press; 1994.p.474-485.

[13] Chung M, Lee J, Park S, Lee M, Lee CE, Lee J, Shin YG. Individual tooth detection and identification from dental panoramic x-ray images via point-wise localization and distance regularization. Artif Intell Med. 2021;111:101996. DOI: 10.1016/j.artmed.2020.101996.

[14] Rashmi S, Murthy P, Ashok V, Srinath S. Cephalometric skeletal structure classification using convolutional neural networks and heatmap regression. SN Comput Sci. 2022;3(5):336. DOI: 10.1007/s42979.022.01230-w

[15] Pizer SM, Amburn EP, Austin JD, Cromatie R, Geselowitz A, Greer T, Romeny BH, Zimmerman JB, Zuiderveld K. Adaptive histogram equalization and its variations. Comput Vision Graph. 1987;39(3):355-368. DOI: 10.1016/S0734-189x(87)80186-X.

[16] Qassim HM, Basheer NM, Farhan MN. Brightness preserving enhancement for dental digital x-ray images based on entropy and histogram analysis. J Appl Sci Eng. 2019;22(1):187-194. DOI: 10.6180/jase.201903_22(1).0019.

[17] Pandyan UM, Arumugam B, Gurunathan U, Kopuli Ashkar Ali SH. Automatic localization of inferior alveolar nerve canal in panoramic dental images. Signal Image Video P. 2022;16(5):1389-1397. DOI: 10.1007/s11760.021.02091-1.

[18] Faul F, Erdfelder E, Lang AG, Buchner A. G*Power 3: a flexible statistical power analysis program for the social, behavioral, and biomedical sciences. Behav Res Methods. 2007;39(2):175-191. DOI: 10.3758/bf03193146.

[19] Koo TK, Li MY. A Guideline of selecting and reporting intraclass correlation coefficients for reliability research. J Chiropr Med. 2016;15(2):155-163. DOI: 10.1016/j.jcm.2016.02.012.

[20] Rossmann K, Wiley BE. The central problem in the study of radiographic image quality. Radiology. 1970;96(1):113-118. DOI: 10.1148/96.1.113.

[21] McWilliam JS, Welander U. The effect of image quality on the identification of cephalometric landmarks. Angle Orthod. 1978;48(1):49-56. DOI: 10.1043/0003-3219(1978)048<0049:TEOIQO>2.0.CO;2.

[22] Döler W, Steinhöfel N, Jäger A. Digital image processing techniques for cephalometric analysis. Comput Biol Med. 1991;21(1-2):23-33. DOI: 10.1016/0010-4825(91)90032-5.

[23] McClure SR, Sadowsky PL, Ferreira A, Jacobson A. Reliability of digital versus conventional cephalometric radiology: A comparative evaluation of landmark identification error. Semin Orthod. 2005;11(2):98-110. DOI: 10.1053/j.sodo.2005.04.002.

[24] Chen YJ, Chen SK, Yao JC, Chang HF. The effects of differences in landmark identification on the cephalometric measurements in traditional versus digitized cephalometry. Angle Orthod. 2004;74(2):155-161. DOI: 10.1043/0003-3219(2004)074<0155:TEODIL>2.0.CO;2.

[25] Turner PJ, Weerakone S. An evaluation of the reproducibility of landmark identification using scanned cephalometric images. J Orthod. 2001;28(3):221-230. DOI: 10.1093/ortho/28.3.221.

[26] Oshagh M, Shahidi SH, Danaei SM. Effects of image enhancement on reliability of landmark identification in digital cephalometry. Indian J Dent Res. 2013;24(1):98-103. DOI: 10.4103/0970-9290.114958.

[27] Duarte H, Vieck R, Siqueira DF, Angelieri F, Bommarito S, Dalben G, Sannomiya EK. Effect of image compression of digital lateral cephalograms on the reproducibility of cephalometric points. Dentomaxillofac Radiol. 2009;38(6):393-400. DOI: 10.1259/dmfr/40996636.

[28] Nikneshan S, Mohseni S, Nouri M, Hadian H, Kharazifard MJ. The effect of emboss enhancement on reliability of landmark identification in digital lateral cephalometric images. Iran J Radiol. 2015;12(2):e19302. DOI: 10.5812/iranjradiol.19302.

[29] Leonardi R, Giordano D, Maiorana F, Spampinato C. Automatic cephalometric analysis. Angle Orthod. 2008;78(1):145-151. DOI: 10.2319/120506-491.1.

[30] Wang CW, Huang CT, Hsieh MC, Li CH, Chang SW, Li WC, Vandaele R, Marée R, Jodogne S, Geurts P, Chen C, Zheng G, Chu C, Mirzaalian H, Hamarneh G, Vrtovec T, Ibragimov B. Evaluation and comparison of anatomical landmark detection methods for cephalometric x-ray images: A grand challenge. IEEE Trans Med Imaging. 2015;34(9):1890-1900. DOI: 10.1109/TMI.2015.241.2951.

[31] Wang CW, Huang CT, Lee JH, Li CH, Chang SW, Siao MJ, Lai TM, Ibragimov B, Vrtovec T, Ronneberger O, Fischer P, Cootes TF, Lindner C. A benchmark for comparison of dental radiography analysis algorithms. Med Image Anal. 2016;31:63-76. DOI: 10.1016/j.media.2016.02.004.

[32] Park JH, Hwang HW, Moon JH, Yu Y, Kim H, Her SB, Srinivasan G, Aljanabi MNA, Donatelli RE, Lee SJ. Automated identification of cephalometric landmarks: Part 1-comparisons between the latest deep-learning methods YOLOV3 and SSD. Angle Orthod. 2019;89(6):903-909. DOI: 10.2319/022019-127.1.

[33] Hwang HW, Park JH, Moon JH, Yu Y, Kim H, Her SB, Srinivasan G, Aljanabi MNA, Donatelli RE, Lee SJ. Automated identification of cephalometric landmarks: Part 2-might it be better than human? Angle Orthod. 2020;90(1):69-76. DOI: 10.2319/022019-129.1

[34] Hwang HW, Moon JH, Kim MG, Donatelli RE, Lee SJ. Evaluation of automated cephalometric analysis based on the latest deep learning method. Angle Orthod. 2021;91(3):329-335. DOI: 10.2319/021220-100.1.

[35] Kumari AR, Rao SN, Reddy PR. Design of hybrid dental caries segmentation and caries detection with meta-heuristic-based ResneXt-RNN. Biomed Signal Process Control. 2022;78:103961 DOI: 10.1016/j.bspc.2022.103961.

[36] Georgieva VM, Mihaylova AD, Petrov PP. An application of dental x-ray image enhancement. In: Dimitrijević T, Stošić B, editors. 13th International Conference on Advanced Technologies, Systems and Services in Telecommunications (TELSIKS); 2017 Oct 18-20; Nis, Serbia; 2017. pp.447-450.

[37] Li W, Jiang X, Sun W, Wang SH, Liu C, Zhang X, Zhang YD, Zhou W, Miao L. Gingivitis identification via multichannel gray-level co-occurrence matrix and particle swarm optimization neural

network. Int J Imaging Syst Technol. 2020;30(2):401-411. DOI: 10.1002/ima.22385.

[38] Rahmi-Fajrin H, Puspita S, Riyadi S, Sofiani E. Dental radiography image enhancement for treatment evaluation through digital image processing. J Clin Exp Dent. 2018;10(7):e629-e634. DOI: 10.4317/jced.54607

[39] Bhan A, Thakur A, Vyas G. Analysis of histogram based compound contrast enhancement with noise reduction method for endodontic therapy. 5th International Conference-Confluence The Next Generation Information Technology Summit (Confluence); 2014 Sept 25-26; Noida, India; 2014. pp.533-537.

[40] Nishimoto S, Sotsuka Y, Kawai K, Ishise H, Kakibuchi M. Personal computer-based cephalometric landmark detection with deep learning, using cephalograms on the internet. J Craniofac Surg. 2019;30(1):91-95. DOI: 10.1097/SCS.000.000.0000004901.

[41] Yao J, Zeng W, He T, Zhou S, Zhang Y, Guo J, Tang W. Automatic localization of cephalometric landmarks based on convolutional neural network. Am J Orthod Dentofacial Orthop. 2022;161(3):e250-e259. DOI: 10.1016/j.ajodo.2021.09.012.

[42] Durão AP, Morosolli A, Pittayapat P, Bolstad N, Ferreira AP, Jacobs R. Cephalometric landmark variability among orthodontists and dentomaxillofacial radiologists: A comparative study. Imaging Sci Dent. 2015;45(4):213-220. DOI: 10.5624/isd.2015.45.4.213

[43] Ha EG, Jeon KJ, Kim YH, Kim JY, Han SS. Automatic detection of mesiodens on panoramic radiographs using artificial intelligence. Sci Rep. 2021;11(1):23061. DOI: 10.1038/s41598.021.02571-x.

[44] Menezes LD, Silva TP, Lima Dos Santos MA, Hughes MM, Mariano Souza SD, Leite Ribeiro PM, Freitas PH, Takeshita WM. Assessment of landmark detection in cephalometric radiographs with different conditions of brightness and contrast using the an artificial intelligence software. Dentomaxillofac Radiol. 2023;52(8):20230065. DOI: 10.1259/dmfr.20230065.

How to cite this article: Gonca M, Sazak Turgut Ç, Gündoğdu Ş. Effects of Contrast Limited Adaptive Histogram Equalization (CLAHE) on Manual and Automated Tracing of Lateral Cephalometric Radiographs. Clin Exp Health Sci 2024; 14: 733-744. DOI: 10.33808/clinexphealthsci.1357008